—研究論文—
Scientific Paper

Seasonal Variation in the Latitude of Geomagnetically Conjugate Points Observed with Imaging Riometers in the Auroral Zone

Yuiti FUJITA[1], Hisao YAMAGISHI[2] and Natsuo SATO[2]

オーロラ帯イメージングリオメータで観測された地磁気共役点緯度の季節変化

藤田裕一[1]・山岸久雄[2]・佐藤夏雄[2]

要旨: 地磁気共役点は固定した点ではなく季節や時刻とともに変動する点だと考えられ，これを実証するため従来から共役点での光学観測によるオーロラ形状の比較が行われてきた．しかし，光学観測では日照や天候の条件のため年間を通じた統計解析は不可能である．本研究では，昭和基地-チョルネス共役観測点に設置されたイメージングリオメータで得られた電離層吸収データを用い，真夜中前のオーロラブレークアップ時に発生する東西に伸びた帯状吸収領域の緯度を比較することにより，共役点位置の季節変化を求めた．約2年間の連続したデータの統計により，以下の特性が明らかにされた．(1) オーロラブレークアップ時の吸収領域の高緯度方向への移動速度は，昭和においてはチョルネスより平均で約15%高い．(2) この時間帯では，アイスランド側に投影された昭和の共役点は，6月頃チョルネスより最も低緯度側，12月頃最も高緯度側に位置する．(3) この季節変化は，IGRF 1995 と Tsyganenko 1989 モデルを組み合わせて用いた計算結果とよく一致する．

Abstract: Seasonal variation in the latitude of geomagnetically conjugate point was obtained statistically using the imaging riometers at Syowa-Tjornes conjugate pair stations. The conjugate point was evaluated experimentally from the relative location of band-type CNA (Cosmic Noise Absorption) appearing at the conjugate stations, associated with auroral breakups in premidnight hours. The statistical analyses were made for poleward moving CNA-bands observed during February 1992 to December 1993. Following characteristics are obtained. (1) The poleward expanding speed of the CNA-bands differs significantly between the two hemispheres: it is faster at Syowa than Tjornes in Iceland by 15% on average. This difference may be attributable to an interhemispherical asymmetry of the magnetic flux tube radii mapped to the ionospheres, which is caused by the differences in the geomagnetic field strength and dip angles between the both stations. (2) The conjugate point of Syowa mapped to the northern hemisphere moves most equatorward in June and most poleward in December from Tjornes.

[1] 総合研究大学院大学極域科学専攻. Department of Polar Science, The Graduate University for Advanced Studies, 9-10, Kaga 1-chome, Itabashi-ku, Tokyo 173-8515.
[2] 国立極地研究所. National Institute of Polar Research, 9-10, Kaga 1-chome, Itabashi-ku, Tokyo 173-8515.

The latitudinal range of the seasonal displacement is about 200 km for the average geomagnetic activities of $Kp=4$. (3) The seasonal displacement agrees well with the calculations of the conjugate points using the combination of IGRF 1995 and Tsyganenko 1989 geomagnetic field models.

1. Introduction

It has been thought that geomagnetic conjugate points are not fixed on the earth, but they move dynamically depending on the external magnetic fields originated from the magnetospheric currents. Both diurnal and seasonal motions of the conjugate points have been theoretically predicted by the field-line mapping method using geomagnetic field models including both internal and external fields (ONO, 1987; TSYGANENKO, 1990). These calculations show that daily motion of the conjugate points forms ellipses elongated in longitudinal direction. The conjugate points of the southern-hemisphere station, mapped to the northern hemisphere, move counterclockwise on these ellipses, if one looks down the motion from the above. The excursion of the diurnal motion becomes largest in solstices and smallest in equinoxes.

On the other hand, conjugate points can be determined experimentally by choosing common structures in auroral forms observed simultaneously at the geomagnetically conjugate stations, since auroral particles precipitate to the northern and southern ionospheres along the geomagnetic field lines, and produce similar forms of visible auroras. DEWITT (1962) analyzed all-sky auroral images at the conjugate pair stations, Campbell Island in the south of New Zealand and Farewell in Alaska ($L=4$), to compare their average luminosity quantitatively. He confirmed the occurrence of similar auroral forms and motions, simultaneous breakups between the two stations. BOND (1969) compared auroral positions between the conjugate pair stations, Buckles Bay in Macquarie Island and Kotzebue in Alaska ($L=5.2$). He found that the auroras were displaced from the nominal conjugate point before breakups, in accordance with the incidence angle of the solar wind to the magnetosphere. BELON *et al.* (1969) analyzed the auroral data obtained by the conjugate aircraft experiment by the University of Alaska (1967-1971), and found that the auroral conjugacy was well maintained in the dipole latitude range of 65°-71° during magnetically quiet period. They also found that the conjugate auroras appeared very close to the calculated conjugate points using only an internal geomagnetic field model. However, the conjugacy did not hold in higher latitudes in the disturbed conditions. STENBAEK-NIELSEN *et al.* (1972) analyzed the data of the conjugate aircraft experiments in a disturbed period, and found that there were two arc systems: one at lower latitudes (inv. lat. 63°-65°) and the other at higher latitudes (inv. lat. $>65°$). The former showed a good conjugacy, while the latter did not. Differences of the auroral motions between the conjugate points were studied by SATO and SAEMUNDSSON (1987) for Syowa Station-Iceland conjugate pair stations. They reported a case that poleward expansions of the auroras were faster for Syowa in Antarctica, although auroral breakup took place almost simultaneously at these stations. The ratio of the poleward expanding speed at Iceland to that of Syowa was 0.6, as was measured from the figure in their paper. FUJII *et al.* (1987) compared large- and small-scale structures of auroras at Syowa-Iceland

conjugate pair stations. They found that the display is not always concurrent for auroras of small-scale (50–100 km) structures, such as rays and curls, although the conjugacy was generally good for large-scale (greater than 100 km) structures and their motions. They suggested that the auroras of large-scale structures and their motions are mainly controlled by certain conditions in the magnetosphere, perhaps near the equatorial region, whereas the small-scale structures are greatly affected by local acceleration processes in the polar high altitudes.

Optical aurora observations on the ground are quite efficient for the study of conjugacy because of their coverage over a large area (*e.g.* all-sky cameras have a field of view of more than 1000 km) and with a high spatial resolution. However, their contributions to conjugate studies are very poor, because either one of the hemispheres is usually sunlit. Even at equinoxes with dark skies at both stations, a weather condition is imposed as another limitation; the sky must be clear at both stations. If one wants to know the conjugacy in summer or winter, to confirm whether the observed results are statistically significant or not, it is necessary to utilize other observational means that can work all through the year. One of such instruments is the radio-wave imager, the imaging riometer.

The riometer (Relative Ionospheric Opacity meter) was developed in 1950's, using a single broad beam antenna. This type of riometer was deployed at the geomagnetically conjugate points located in sub-auroral zone, auroral zone and polar cap in 1960's (*e.g.*, HOOK, 1962; HARGREAVES and CHIVERS, 1965; HARGREAVES and COWLEY, 1967). Their spatial resolutions were limited by the separations between the stations.

Multi-directional beam riometers became available in late 1960's. HARGREVES (1969a) estimated the position of the absorption regions observed by 5-beam riometers installed at the conjugate pair stations, Great Whale River in Canada and Byrd Station, Antarctica (approximately $L=7$). He assumed that the absorption region was expressed by a two-dimensional gaussian-function, which had spatial scales of 250 km in latitude and 320 km in longitude. He found that the conjugate point of the southern station projected to the northern hemisphere shifted most poleward in northern winter and most equatorward in northern summer in midnight hours, and just in the opposite way in midday hours.

In late 1980's, the riometer equipped with two-dimensional array antennas became available to obtain absorption images (DETRICK and ROSENBERG, 1990), and this system was called the imaging riometer, or simply as IRIS (Imaging Riometer for Ionospheric Studies). The IRIS can observe the absorption regions and their motions in 200 km square at the absorption layer altitude of 90 km, with a spatial resolution of 20 km near the zenith. A pair of imaging riometers was installed at Syowa Station, Antarctica and Tjornes in Iceland (YAMAGISHI *et al.*, 1992). In this paper we will call this system as SIRACE (Syowa-Iceland Radiowave Absorption Conjugacy Experiment) (YAMAGISHI *et al.*, 1998).

The purpose of this study is to find the conjugate characteristics of auroral display, in particular the seasonal variations of the conjugate points and their excursion range. We examine a latitudinal motion of the conjugate points using absorption events observed by SIRACE. We concentrate particularly on poleward expanding absorption bands elongated in the east-west direction, associated with auroral breakups. The statistical analyses are carried out for the band-type absorption events observed during February 1992 to December 1993. The characteristics are compared with model calculations of the conju-

gate points using IGRF 1995 and Tsyganenko 1989 models.

2. Observation System

SIRACE consists of a pair of imaging riometers near conjugate points, Syowa Station in Antarctica and Tjornes in Iceland, in the auroral zone. Both imaging riometers are equipped with two-dimensional 64-beam array antenna. Figure 1 shows the projection of the antenna beams to an absorption layer altitude of 90 km. This figure shows that the field of view is approximately 200 km square, and the spatial resolution is 20 km near the zenith. The observations at Tjornes started in July 1990 and at Syowa in February 1992. Ever since, the observations have been continued with a sampling interval of 4 and 1 s/frame, respectively. Table 1 shows the geographic coordinates of the both stations and their conjugate points, and the L-values of the stations.

The data of cosmic radio noise intensities received by the array antenna are stored on magneto-optical disks. Figure 2a shows a time-series of noise intensity images observed at Tjornes. The accumulated data are processed to obtain a reference level of the galactic noise distribution, which we call as QDN (Quiet Day Noise) images in this paper. When auroras appear, the D-region ionosphere suffers an excess ionization by precipitating energetic auroral electrons. This ionization brings in an increased ionospheric absorption of the cosmic noise. In this way, the cosmic noise intensities in the portion of the sky illuminated by auroras are decreased, as marked by arrows in Fig. 2a. By subtracting the QDN images from these radio noise images, we can obtain images of auroras in the form of the ionospheric absorption, as shown in Fig. 2b. These processes are performed with a personal computer in real-time basis at the observation site (SATO *et al.*, 1992).

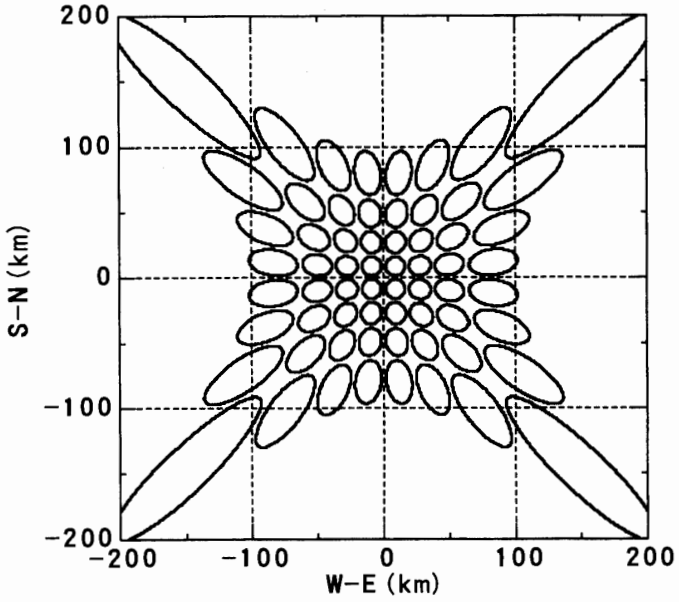

Fig. 1. Projection of 64 antenna-beams formed by 8 by 8 half-wavelength dipoles to the ionospheric absorption altitude of 90 km.

Table 1. Geographic coordinates of the stations and the conjugate points, and geomagnetic parameters calculated by IGRF 1995 model.

Station	Symbol	Geographic		Conjugate*		*L*-value	MLT-UT
		Latitude	Longitude	Latitude	Longitude		
Syowa	SYO	−69.00	39.58	65.58	341.49	6.16	2 (min)
Tjornes	TJO	66.20	342.88	−68.96	42.00	6.39	7 (min)

*At 90 km altitude.

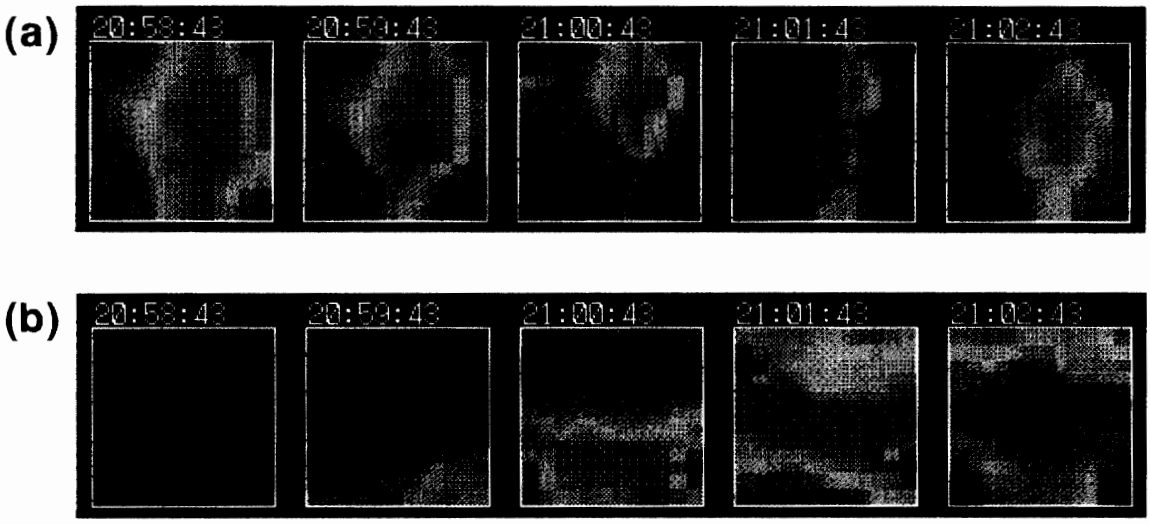

Fig. 2. Upper panel (a) shows a series of galactic noise images observed at Tjornes. Arrows show the portion where the galactic noise was absorbed by an excess D-region ionization associated with auroral appearance. Lower panel (b) shows a series of CNA images obtained from the galactic noise by subtracting background quiet-day noise.

3. Conjugate Point Calculated with Geomagnetic Field Models

Figure 3 shows the field of view of the imaging riometer at Tjornes (TJO) and that of Syowa mapped to the northern hemisphere along magnetic field line (C-SYO), calculated with IGRF 1995 model (hereafter, we call IGRF 1995 model simply as IGRF model). The conjugate field of view for Syowa is reduced in north-south direction by 30% than that for Tjornes. This reduction is due to smaller dip angle of Syowa (66°) than that of Tjornes (77°), and smaller magnetic field intensity at Syowa (~42100 nT) than at Tjornes (~50300 nT). This difference on the fields of view causes an apparent difference in the spatial-scale and the motions of ionospheric absorption observed at Syowa and Tjornes. For example, latitudinal velocities of the energetic electron precipitation regions in the polar ionosphere, which reflects the motions of the electron sources in the magnetosphere, become faster for the southern hemisphere (Syowa) than the northern hemisphere (Tjornes) by ~30%.

In the magnetic field line tracing, the effect from the external field cannot be neglected, especially when the field line extends deep into the magnetosphere. Therefore, in the field-line tracing in high latitudes, it is essential to introduce an external magnetic field such as given by Tsyganenko 1989 model (TSYGANENKO, 1989, hereafter, referred to as T89

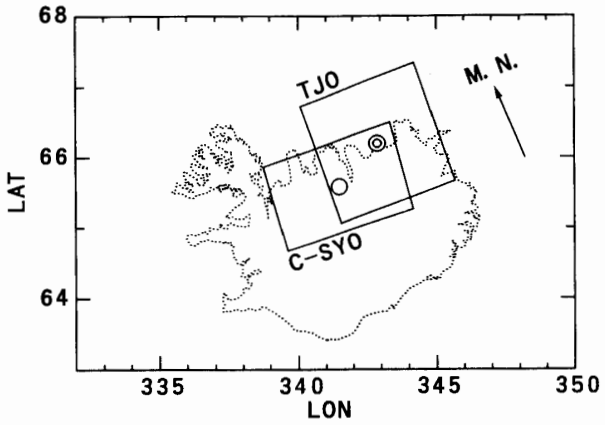

Fig. 3. Field of view of the imaging riometer at Tjornes (TJO) and that of Syowa mapped onto Iceland (C-SYO) by field-line tracing using internal magnetic field model (IGRF). Both field of views are displayed at an altitude of 90 km.

model), together with the internal magnetic field model (IGRF model). Results of the calculation are shown in Fig. 4, in the same format as Fig. 3, for 4 magnetic local times of 00, 06, 12, and 18 h. It is found that the conjugate fields of view of Syowa, mapped onto the northern hemisphere, are deformed in longitudinal direction. This indicates that the external field causes a larger longitudinal displacement in higher latitudes. This displacement may be caused by a tailward stretching of the field lines on the frank side of the magnetosphere by the solar wind. This deformation causes a difference between absorption areas observed at Tjornes and Syowa. For example, the absorption area elongated in the north-south direction at Syowa is deformed to a northeast-southwest or northwest-southeast elongated area at Tjornes. On the other hand, the absorption area elongated in east-west direction at Syowa remains the same east-west area at Tjornes.

The deformation of the fields of view also causes the velocity difference of conjugate

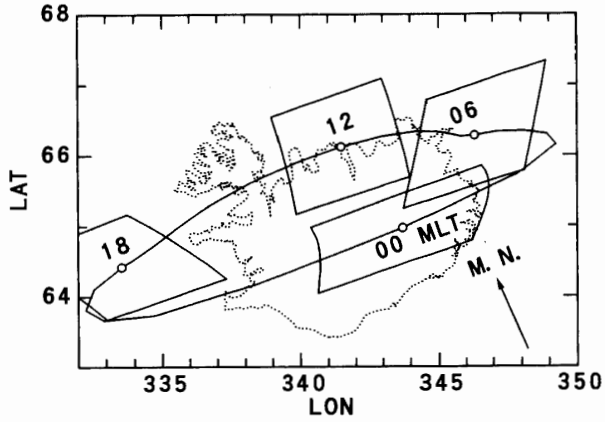

Fig. 4. Field of views of the Syowa imaging riometer mapped onto Iceland by field-line tracing using both the internal field (IGRF) and external field model (T89) for different local times of 00, 06, 12 and 18 MLT.

absorption regions moving in the north-south direction between the both stations. Thus, the ratios of the poleward expanding velocities at Tjornes to that at Syowa depend on magnetic field models. If we employ IGRF and T89 models for $Kp=4$ in June, the ratios are;

$$\begin{aligned} R_{\text{model}} &= V_t / V_s, \\ &= 0.7 \text{ (IGRF internal field only)}, \\ &= 0.7 \text{ (IGRF+T89 at 18 MLT)}, \\ &= 0.6 \text{ (IGRF+T89 at 00 MLT)}, \end{aligned} \tag{1}$$

where R_{model} is ratio between the poleward expanding velocities, V_t, V_s are poleward expanding velocities observed at Tjornes and Syowa.

Figure 5 (a-d) shows trajectories of the diurnal motions of the conjugate points of Syowa for different seasons of the year calculated with the combination of IGRF and T89 models for $Kp=0$. The latitudinal excursion of the diurnal motion becomes largest at

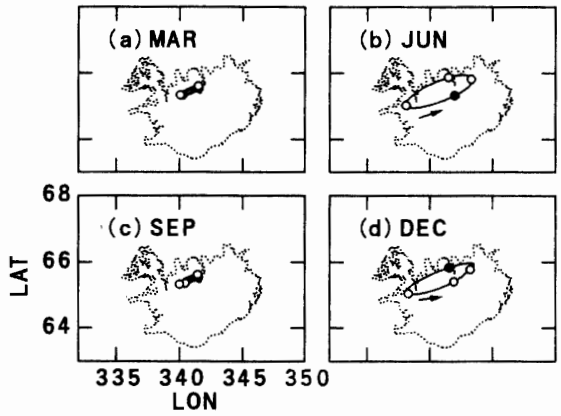

Fig. 5. Diurnal displacement of the conjugate points of Syowa for four seasons (March, June, September and December) in 1992. They are calculated using both the internal (IGRF) and external (T89) field models and projected at an altitude of 90 km for Kp=0. (Full circles mean 00 MLT, white ones mean 06, 12, 18 MLT.)

solstices and smallest at equinoxes. The conjugate points rotate counterclockwise if one looks down the motion from the above. Figure 6 shows diurnal motions in June 1992 as a function of Kp indices. The excursion of the diurnal motion becomes greater as Kp index increases. Here, we concentrate on the seasonal variation of the conjugate points near midnight hours, in which band-type absorption most frequently occurs. In Fig. 7, we show the seasonal variation of the conjugate points at midnight (00 MLT). It is clearly found that the conjugate point shifts most equatorward in June and most poleward in December. Excursion range of this seasonal variation is about 200 km in latitude and 100 km in longitude for $Kp=4$.

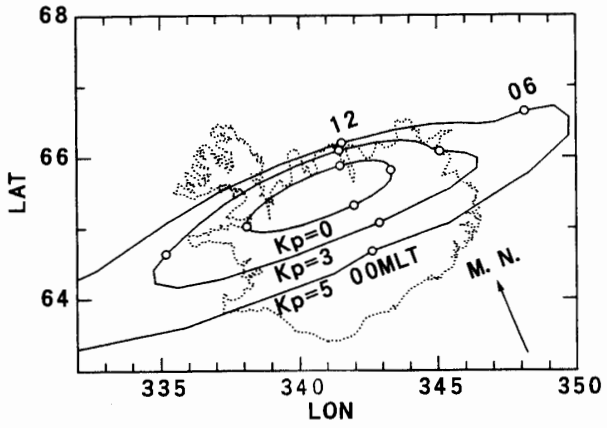

Fig. 6. Diurnal displacements of the conjugate points of Syowa for Kp=0, 3 and 5 for June 1992. They are calculated using both internal (IGRF) and external (T89) field models. The displacements are projected at an altitude of 90 km.

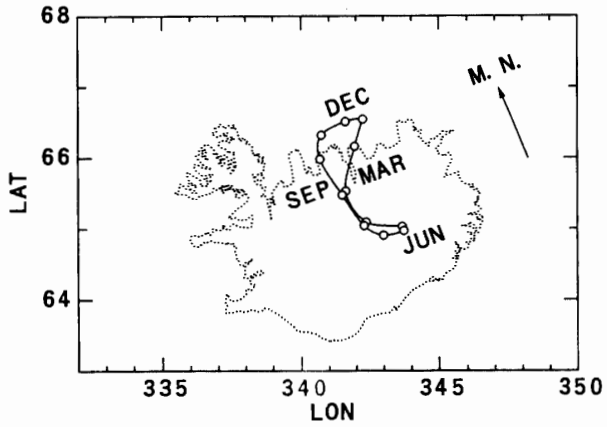

Fig. 7. Seasonal variation in the conjugate points of Syowa at 00 MLT for Kp=4. It is calculated using both internal (IGRF) and external (T89) field models and projected at an altitude of 90 km.

4. Data Analysis

If one wants to examine 'point to point' conjugacy in SIRACE observation, it is necessary to find out common characteristic structures appearing at the both stations. Unfortunately, the imaging riometers have a narrower field of view (200 km square) and poorer spatial resolution (20 km near zenith) compared with all-sky cameras. Therefore, we select absorption features with a simple form such as a band-type. Figure 8 shows an example of the band-type absorption observed simultaneously at Tjornes (upper panel) and Syowa (lower panel). Hereafter, this type of the absorption event is abbreviated to PECB (Poleward Expanding CNA Band).

PECBs are usually associated with onsets of auroral substorms, and usually show a good conjugacy between the two hemispheres. They show relatively a large absorption intensity of several dB and have band-type structures elongated in east-west direction, and

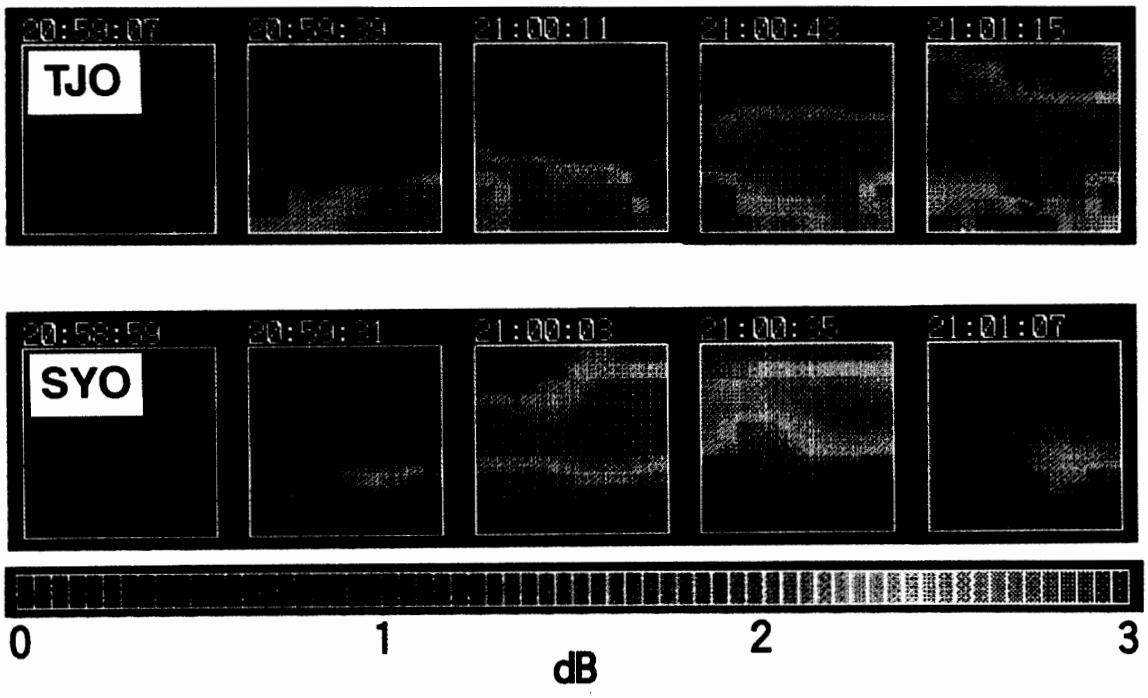

Fig. 8. Poleward expanding CNA band (PECB) observed on February 18, 1993 at Tjornes (upper panel) and Syowa (lower panel).

move poleward at a speed of several hundred m/s to a few km/s, passing the fields of view of the imaging riometers in a few minutes. Subsequently, they are soon (~10 min) followed by CNA bands coming back to lower latitudes. At this stage, the conjugacy becomes very poor, possibly due to the distorted magnetosphere configuration caused by enhanced field-aligned currents, which do not flow symmetrically in the both hemispheres. It often takes more than an hour before the conjugacy is recovered. At the recovery phases of substorms, CNAs of irregular shapes, such as patchy structures, appear at the both observatories. It is usually difficult to find out one-to-one correspondence of CNA patches, because of an ambiguity of the patchy structures between the two hemispheres. Therefore, it is most promising to analyze PECBs for studying the conjugacy. Analysis was carried out with the following procedure.

4.1. Event selection

Figure 9 shows some meridional plots we produced from our CNA image data, where CNA intensities are averaged for 30 s to reduce random noise. Using these meridional plots, PECBs appearing at the both stations are selected under the following criteria.

(1) CNA intensities at either station must be larger than 1dB at their maximum, in order to pick up pronounced CNA events.

(2) The time difference of PECBs crossing the zenith must be less than 300 s between the two stations.

(3) Similar type of CNA must not precede within 30 min before the onset of each selected PECB, in order to avoid a possible influence from the preceding events.

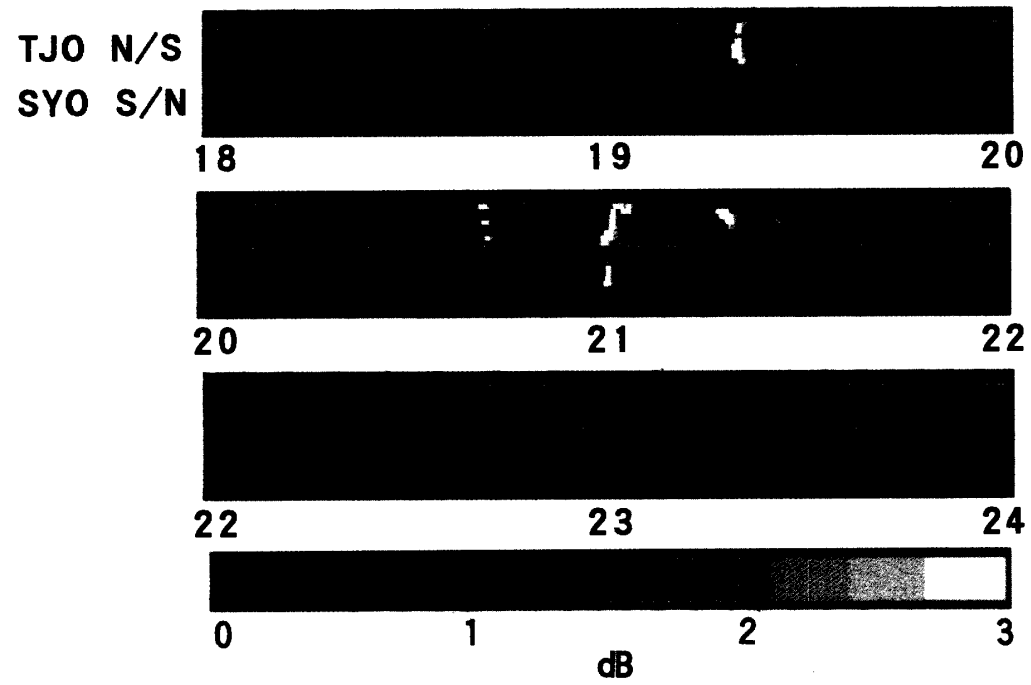

Fig. 9. A series of meridional plots of CNAs observed on February 18, 1993 at Tjornes and Syowa. Note that PECB appeared at 21 UT at the both stations.

It is generally difficult to distinguish the following two cases: (a) the same event, but appeared with some time lag between the two fields of view, (b) the different events, but appeared with a short time lag between the two fields of view. In order to reduce the possibility of including the latter case, we adopt criterion (2).

The model calculations tell us that the seasonal variation of the conjugate points is strongly dependent on local time. Therefore, in the data analysis, it is important to select a most suitable time-window to obtain pronounced seasonal characteristics. We first check local-time distribution of PECB occurrence, thereafter we select the time-window showing the most frequent occurrence.

4.2. Determination of the poleward expanding velocities and conjugate point locations

In order to obtain the poleward moving velocity and zenith crossing time of PECBs, we utilize meridional plots with expanded time scale (Fig. 10). The black solid-curves in the center of the each plot of Fig. 10 represent the trace of the peaks of the PECBs. Since the separation of the IRIS-beams increase toward the edge of the field of view, as shown in Fig. 1, the trace of the PECBs with a constant velocity becomes 'S' shape, rather than a straight line. The cross marks '+' on the curves represent the zenith crossing times. The poleward moving velocities at Tjornes and Syowa are denoted by V_t, V_s, and their zenith crossing times by T_t and T_s, respectively. Here we assume that the PECBs move with a constant velocity, as shown schematically in Fig. 11a. Figure 11b illustrates that latitudinal displacement 'D', of the conjugate point of Syowa from Tjornes, is obtained from the poleward expanding velocity 'V' and the difference between the both zenith

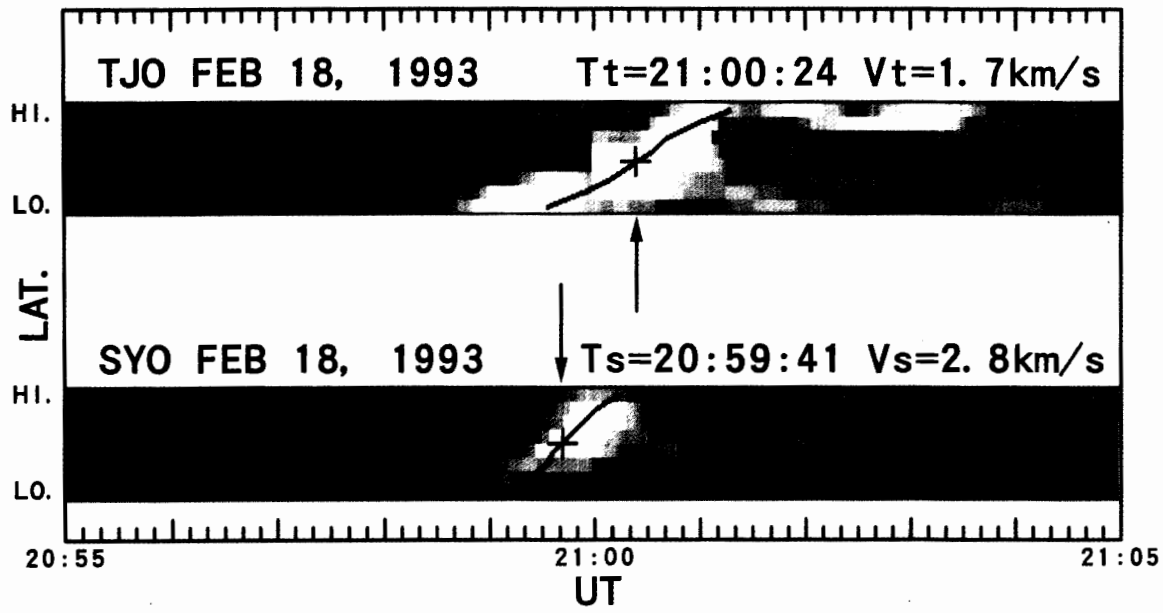

Fig. 10. An expanded plots of the PECB meridional shifting to determine the poleward moving velocities, V_t and V_s, and the zenith crossing times, T_t and T_s. The velocities and the times are determined by linear fitting, assuming the velocity to be constant and the form of CNA region unchanged.

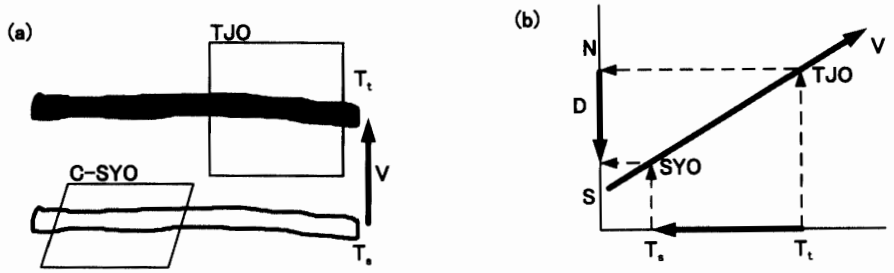

Fig. 11. Illustrations to show how the zenith crossing time of PECBs, and the latitudinal displacement of the conjugate point of Syowa from Tjornes are determined from the absorption images. (a) The zenith crossing time at Tjornes and Syowa is given as T_t and T_s, assuming a constant poleward expanding velocity (V) of PECB. V is the mean of the observed velocities at Tjornes and Syowa. (b) Latitudinal displacement of Syowa conjugate point from Tjornes, D, is determined by the poleward expanding velocity, V, and the interval of the zenith crossing time of the both stations, T_s-T_t.

crossing times of PECBs, T_t and T_s. The displacement D is expressed by the following relation.

$$D = V\ (T_s - T_t). \quad \text{(positive for poleward)} \tag{2}$$

Where V is poleward-expanding velocity, T_s is zenith-crossing time at Syowa, T_t is zenith-crossing time at Tjornes.

There is a problem how to determine V from V_t and V_s denoted by eq. (1). Because, V_t and V_s are usually different, or more correctly, V_s exceeds V_t by ~30% according to the model calculations described in Section 3. We assume V in the northern hemisphere as a mean of V_t and V_s', where V_s' is the value of V_s mapped to the northern hemisphere. As a mapping factor of V_s, we take average value of the observed velocity ratios, 'R_{obs}'. These relationships are expressed by following equations.

$$V=(V_t+V_s')/2=(V_t+R_{obs}V_s)/2, \tag{3}$$

$$R_{obs}=10^{[\log(V_t/V_s)]}, \tag{4}$$

where $[\log(V_t/V_s)]$ represents average of $\log(V_t/V_s)$ for all the selected events.

It must be noted here that the velocity ratios are averaged in logarithmic scale, not in linear scale. The reason is as follows. The velocity ratio (V_t/V_s) for each event has a value of 0 to 1, or 1 to infinity, depending on V_t is smaller or larger than V_s, respectively. If we directly average V_t/V_s, the average value tends to be much greater than 1, biased by predominant cases of $V_t > V_s$. Hence, we first take the average of $\log(V_t/V_s)$, thereafter, convert the average value, $[\log(V_t/V_s)]$, to linear scale by calculating $10^{[\log(V_t/V_s)]}$. As the result, R_{obs} is determined to be 0.85, which is a little larger than the calculated value (~0.7) of V_t/V_s with the combined IGRF and T89 models for the geomagnetic field.

4.3. Cosine curve fitting of the seasonal displacement of conjugate points

In the previous section, we described how to obtain the latitudinal displacement of the conjugate point using the meridional plots of PECB events. In order to compare the theoretical latitudinal displacement shown in Fig. 7 with the observed one, we modify the displacement of Fig. 7 to the latitudinal displacement with month in Fig. 12. This variation is approximately expressed by a cosine curve, as follows.

$$d(t)=d_0+A\cos\{2\pi(t-t_0)/365\}, \tag{5}$$

where $d(t)$ is the latitudinal displacement of the conjugate points, t is day of the year, t_0 is day of the year showing the maximum displacement, A is amplitude of the displacement

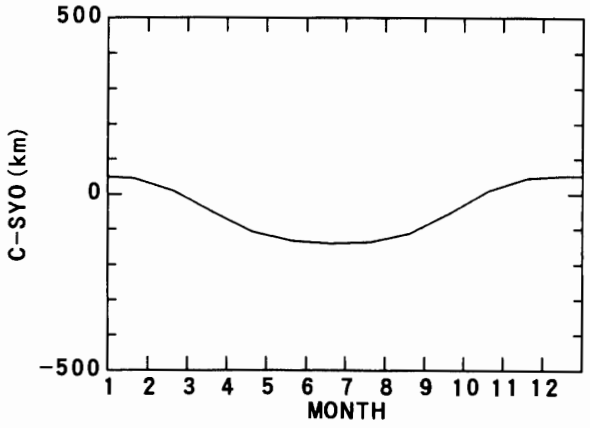

Fig. 12. Seasonal variation in the latitudinal displacement of the conjugate point of Syowa from Tjornes (denoted by C-SYO) calculated with IGRF and T89 field models for 00 MLT.

within a year, d_0 is average displacement of Syowa conjugate points from Tjornes. This function is used as a fitting curve for the observed displacements of the conjugate point to investigate the seasonal characteristics such as the variation amplitude, and the time of the maximum displacement.

5. Conjugate Analysis of PECB Events

We analyze 92 PECB events observed simultaneously at Syowa and Tjornes from February 1992 to December 1993. Figure 13 shows the occurrence dependence on magnetic local time. Nearly 60% of the events occur within 3 hours prior to the magnetic midnight. As discussed in Section 4.1, the seasonal variation of the conjugate point is so strongly dependent upon local time that we select the events in the time-window of 21-24 MLT showing the most frequent occurrence, in order to obtain pronounced seasonal characteristics. Following results are obtained.

(1) Interhemispherical difference of poleward expanding velocities

Figure 14 shows an occurrence histogram of the ratios of poleward expanding velocities of PECBs at Tjornes to those at Syowa. The velocity ratios (V_t/V_s) range from 0.4 to 1.9 excluding the one exceptionally large ratio of 2.5. The abscissa is scaled in logarithmic, as explained in Section 4.2. The mean velocity ratio (V_t/V_s) is 0.85, indicating that the poleward expanding velocity is faster at Syowa than Tjornes.

(2) Latitudinal displacement of the conjugate points

Latitudinal displacements of the conjugate point of Syowa from Tjornes are examined for 55 conjugate PECB events occurred in the time-window of 21-24 MLT, according to Section 4.3, and the displacements are plotted in Fig. 15 as a function of the time of the year. The best-fit cosine curve, mentioned in Section 4.3, is also displayed in this figure. Although the plots show a large scatter, we can find a clear tendency that the conjugate points of Syowa shift equatorward in June and poleward in December. Latitudinal range of the seasonal displacement, represented by the amplitude (A) of the fitted curve, is about

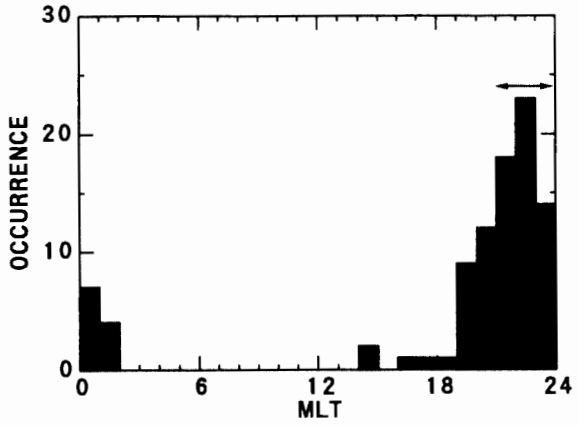

Fig. 13. Local time dependence of the occurrence of PECB events observed simultaneously at Tjornes and Syowa. The arrow shows the time window which the event most frequently occurred.

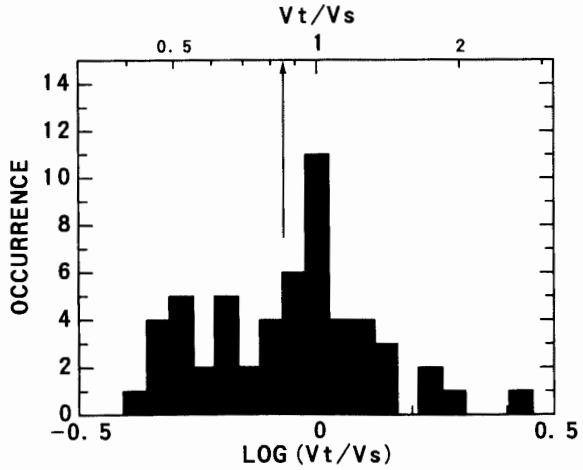

Fig. 14. Distribution of the interhemispherical velocity ratios of PECB events occurred in 21–24 MLT. An arrow shows the mean value (0.85) of the velocity ratios.

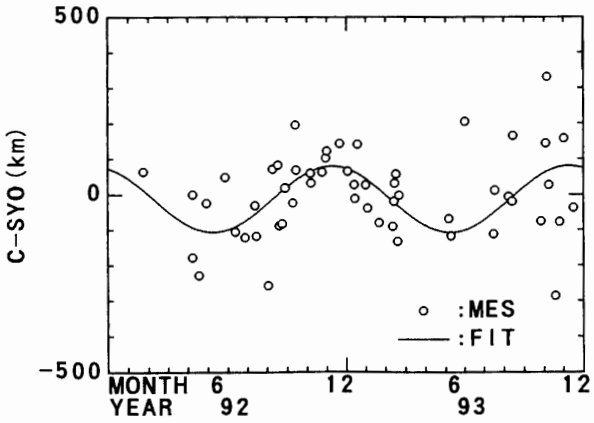

Fig. 15. Seasonal variation in the latitudinal displacement of Syowa conjugate point from Tjornes for conjugate PECB events occurred in 21–24 MLT (circles). Solid curve is a cosine fitting curve determined by the least mean square method.

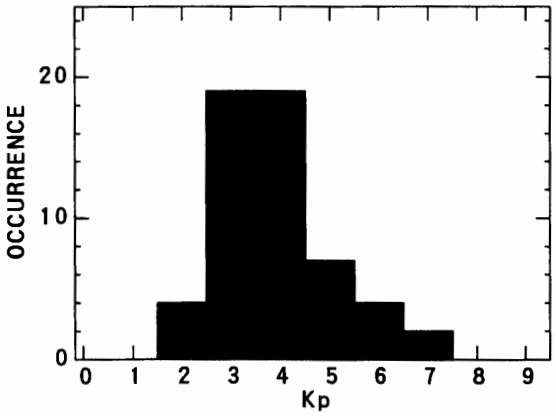

Fig. 16. Kp-dependence for 55 PECB events shown in Figs. 14 and 15. The mean Kp value was 4.

100 km.

(3) Geomagnetic activity dependence of the PECBs

Figure 16 shows the occurrence histogram of 55 PECBs against *Kp* indices. The mean value of the *Kp* indices for these events is 4, and the standard deviation is 1. This indicates that the analyzed PECBs occurred during moderate geomagnetic disturbances.

6. Discussions

6.1. Velocity ratio of the event between hemispheres

SATO and SAEMUNDSSON (1987) showed that the velocity of auroral poleward expansion was different between the conjugate stations, using ground-based scanning photometers at Syowa in Antarctica and Husafell in Iceland. The velocity ratio (V_t/V_s) was approximately 0.6 (as measured from their Fig. 3). In this study, we obtain that the velocity ratios of PECBs are from 0.4 to 2.5. However, if we take only the confidence interval with 95% reliability, the velocity ratios are limited within 0.78 and 0.94, and the median value is 0.85 when the gaussian-distribution is assumed. Thus, we can reach a significant conclusion that the poleward expansion at Syowa is statistically faster than at Tjornes. The observed average velocity ratio, 0.85, is slightly larger than the ratio of 0.7 calculated from IGRF and T89 models. In order to give a reasonable physical interpretation for this interhemispheric velocity difference, we show a simple discussion based on a flux tube model shown in Fig. 17, where we estimate the interhemispheric differences arising from the magnetic field strengths and dip angles. We assume a flux tube having a circular cross section on the equatorial plane in the magnetosphere. The cross section of this flux tube changes to ellipses elongated in latitudinal direction in the northern and southern ionospheres. Here we compare the latitudinal radii of the cross sections between the two hemispheres. The ratio of the radius is given by the following equation.

$$\frac{R_t}{R_s}=\sqrt{\frac{B_s \sin (I_s)}{B_t \sin (I_t)}}=0.89, \tag{6}$$

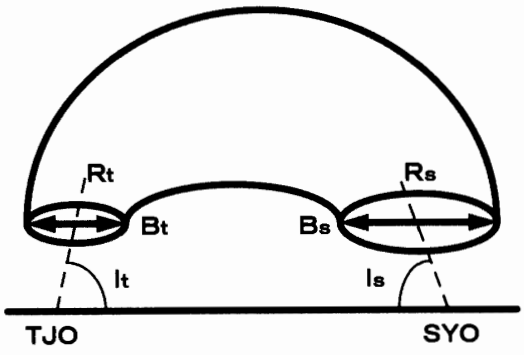

Fig. 17. An illustration of the model flux tube connecting Tjornes and Syowa. Differences in dip angle at the both stations, I_t and I_s, and magnetic field intensity, B_t and B_s, causes a slight but noticeable difference in the radii of the tube at the both foot points, R_t and R_s.

where, R_t, R_s are latitudinal radii of the flux tube at the ionosphere above Tjornes and Syowa, respectively, I_t, I_s are dip angle at Tjornes and Syowa, respectively, B_t, B_s are geomagnetic field strength at Tjornes and Syowa, respectively.

During the PECB events, the field strengths and the dip angles may deviate from their quiet-time values by only a few percent and one degree, respectively. Such a small deviation will not affect the R_t/R_s calculation with eq. (6). However, the flux tube model must be applicable not only during quiet times, but also in disturbed times when PECBs predominantly occur. The ratio of the radius, $R_t/R_s=0.89$, is equivalent to the velocity ratio of a PECB. This model value is rather close to the observed ratio of 0.85, compared to the predicted ratio of 0.7 with IGRF and T89 models. This will indicate that the magnetospheric configuration at the expansion onset is not actually deformed as predicted by IGRF and T89 models at the stage of PECB occurrence.

6.2. Seasonal displacement of the conjugate point of Syowa

In Section 5, we have obtained the seasonal variation in the conjugate points of Syowa in 21–24 MLT from PECBs at Syowa and Tjornes. We found that the conjugate points shift most equatorward in June and most poleward in December. The displacement by the cosine fitted curve is estimated to be approximately 100 km in latitudinal direction. The *Kp*-index for these events was 4 on average. The seasonal variation of the conjugate points calculated with IGRF and T89 models on the same magnetic local time and *Kp*-index (Fig. 12), agrees considerably well with the cosine curve fitted to the analyzed displacements (Fig. 15) in both the phase and the amplitude. The seasonal variation of the conjugate points may be due to the seasonal change in the incidence angle between the solar wind flow direction and the geomagnetic dipole axis.

As described above, HARGREAVES (1969a) estimated the positions of conjugate CNAs assuming the spatial distributions of absorption, from the conjugate observations using 5 broad-beam riometers located near $L=7$. The assumption is two-dimensional gaussian-distributions of CNA regions with an extent of 250 km in latitude and 320 km in longitude. He compared the center positions of the CNA regions between the both hemispheres with 1-min time-resolution. As the result, he found that the conjugate points of Byrd projected to the northern hemisphere are displaced most equatorward in northern summer and most poleward in northern winter during nighttime, which result is consistent with ours. The events analyzed during nighttime were mostly spiky events shorter than 10-min duration. The PECBs we have analyzed are regarded as a subset of the spiky events. He also observed the width of the seasonal variation to be approximately 100 km in latitude, which is nearly the same as the one in this study. These results also agree with the calculations with IGRF and T89 models. This agreement with the observations supports the validity of the geomagnetic field models, at least, for long-term variations such as seasonal displacement of conjugate points.

This study concentrated on the PECB events during nighttime. On the other hand, in daytime, larger-scale structures of drifting CNA are observed. Since the size of the structure is nearly equal to the field of view of the imaging riometers, it seems to be difficult to compare the corresponding structures between the both stations. Further studies for daytime conjugacy will be required.

6.3. *Scattering of Syowa conjugate point*

The latitudinal displacements of conjugate points are scattered near the fitted cosine curve, as shown in Fig. 15. The displacements are obtained from the events in the time interval of 21-24 MLT, for average *Kp*-index of 4. Since locations of the conjugate points are highly dependent upon local time and *Kp*-index in the T89 model, the variations for magnetic local times and *Kp*-indices would cause the scatter of the conjugate points. In order to estimate the amount of this scatter, we calculated monthly variation in the latitudinal displacement of the conjugate points with various local times during 21-24 MLT and *Kp*-index in $3 < Kp < 5$, and the result is shown in Fig. 18. The maximum scatter of the displacement is estimated to be 50 km, centered at the seasonal curve shown in Fig. 12. On the other hand, the observed scatter shown in Fig. 15 is mostly within 50 km, and some points show much larger deviation from the fitted curve. This suggests that the configuration of the magnetosphere is influenced by transient changes that cannot be expressed by the static magnetosphere models.

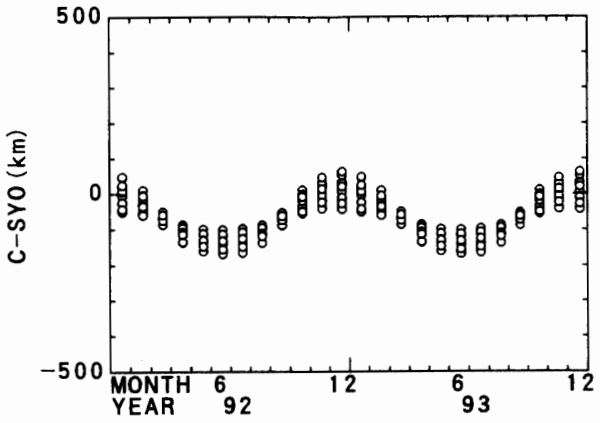

Fig. 18. Scatter plot of the conjugate points of Syowa calculated with IGRF and T89 models in 1992 and 1993 for various local times in the interval of 21-24 MLT and Kp values of $3 < Kp < 5$. The scatter of the conjugate points is mostly within 50 km of the fitted cosine curve shown in Fig. 15.

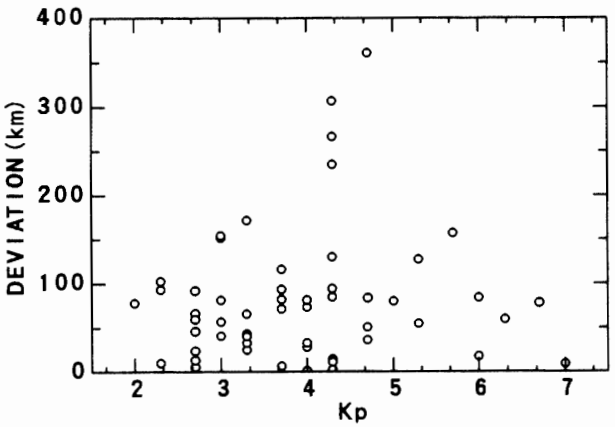

Fig. 19. Kp-dependence of the latitudinal displacement of the conjugate points of Syowa from Tjornes.

Figure 19 shows the latitudinal deviations from the fitted curve with Kp indices from Fig. 15. Most of the deviations are in the range of less than 100 km for various Kp-values, which correspond to the scatter from the model calculation shown in Fig. 18. The deviations also show increase with Kp indices up to $Kp=5$, but the increasing trend is not clear above $Kp=5$ because of the small number of events. Since CNA occur frequently with geomagnetic disturbances, the decrease of the conjugate PECB occurrence in $Kp\geqq 5$ may be caused by a break down of conjugacy due to larger distortion of the magnetosphere configuration. Therefore, the two imaging riometers could not identify the same event.

HARGREAVES (1969b) showed that there was no apparent relationship between conjugacy and geomagnetic disturbance. He used 5 sets of broad-beam riometer, and assumed the extent of CNA region to be 250 km in latitude and 320 km in longitude. This size is comparable to the width of auroral zone. On the contrary, in our study, the conjugacy becomes poor in the severely disturbed period ($Kp\geqq 5$), as shown in Fig. 19. The latitudinal width of PECB regions observed by SIRACE is an order of tens of kilometer, which is the order of each element of auroral arc. The result in the conjugacy-geomagnetic disturbance relationship by HARGREAVES may be caused by his assumption for the shape of CNA regions.

7. Conclusion

Seasonal variation in geomagnetically conjugate point of Syowa Station, Antarctica is investigated statistically using the CNA data obtained by SIRACE. The statistical analyses are carried out for east-west elongated poleward expanding CNA band (PECB) with local auroral breakups in premidnight hours from February 1992 to December 1993. Following characteristics are obtained.

(1) Poleward expanding speed of CNA bands is faster for Syowa than Tjornes by 15% on average.
(2) The conjugate points of Syowa, which were determined experimentally, displace most equatorward in June and most poleward in December. The latitudinal range of this seasonal variation is about 200 km for moderate geomagnetic disturbances of $Kp=4$.
(3) The seasonal variation of the conjugate points agrees well with that expected from the calculations with IGRF and T89 models for $Kp=4$.

Acknowledgments

The authors wish to express their appreciation to the members of the 33rd and 34th Japanese Antarctic Research Expedition for the construction and operation of the imaging riometer at Syowa Station. They also express their thanks to Prof. Th. SAEMUNDSSON, University of Iceland, for his support in operating imaging riometer at Tjornes. The model calculations were made using software prepared by Mr. A. KADOKURA, WDC C2 for aurora in NIPR. Authors express their appreciation to the members of Upper Atmospheric Physics division of NIPR for their valuable discussions and encouragement. The project in Iceland was supported by the Monbusho International Scientific Research Program (04044165, 0744104).

References

BOND, F.R. (1969): Auroral morphological similarities at two magnetically conjugate stations: Buckles Bay and Kotzebue. Aust. J. Phys., **22**, 421–433.

BELON, A.E., MAGGS, J.E., DAVIS, T.N., MATHER, K.B., GLASS, N.W. and HUGHES, G.F. (1969): Conjugacy of visual auroras during magnetically quiet periods. J. Geophys. Res., **74**, 1–28.

DETRICK, D.L. and ROSENBERG, T.J. (1990): A phased-array radiowave imager for studies of comic noise absorption. Radio Sci., **25**, 325–338.

DEWITT, R.N. (1962): The occurrence of aurora in geomagnetically conjugate areas. J. Geophys. Res., **67**, 1347–1352.

FUJII, R., SATO, N., ONO, T., FUKUNISHI, H., HIRASAWA, T., KOKUBUN, S., ARAKI, T. and SAEMUNDSSON, TH. (1987): Conjugacy of rapid motions and small-scale deformations of discrete auroras by all-sky TV observations. Mem. Natl Inst. Polar Res., Spec. Issue, **48**, 72–80.

HARGREAVES, J.K. (1969a): Conjugate and closely-spaced observations of auroral radio absorption-1. Planet. Space Sci., **17**, 1459–1484.

HARGREAVES, J.K. (1969b): Conjugate and closely-spaced observations of auroral radio absorption-2. Planet. Space Sci., **17**, 1485–1495.

HARGREAVES, J.K. and CHIVERS, H.J.A. (1965): A study of auroral absorption events at the South Pole. J. Geophys. Res., **70**, 1093–1102.

HARGREAVES, J.K. and COWLEY, F.C. (1967): Studies of auroral radio absorption events at three magnetic latitudes-2. Planet. Space Sci., **15**, 1585–1597.

HOOK, J.L. (1962): Some observations of ionospheric absorption at geomagnetic conjugate stations in the auroral zone. J. Geophys. Res., **67**, 115–122.

ONO, T. (1987): Temporal variation of the geomagnetic conjugacy in Syowa-Iceland pair. Mem. Natl Inst. Polar Res., Spec. Issue, **48**, 46–57.

SATO, M., YAMAGISHI, H., KATO, Y. and NISHINO, M. (1992): Quick-look system of auroral absorption images by imaging riometer. Nankyoku Shiryô (Antarct. Rec.), **36**, 251–267 (in Japanese with English abstract).

SATO, N. and SAEMUNDSSON, TH. (1987): Conjugacy of electron auroras observed by all-sky cameras and scanning photometers. Mem. Natl Inst. Polar Res., Spec. Issue, **48**, 58–71.

STENBAEK-NIELSEN, H.C., DAVIS, T.N. and GLASS, N.W. (1972): Relative motion of auroral conjugate points during substorms. J. Geophys. Res., **77**, 1844–1858.

TSYGANENKO, N.A. (1989): A magnetospheric magnetic field model with a warped tail current sheet. Planet. Space Sci., **37**, 5–20.

TSYGANENKO, N.A. (1990): Quantitative models of the magnetospheric magnetic field: method and results. Space Sci. Rev., **54**, 75–186.

YAMAGISHI, H., NISHINO, M., SATO, M., KATO, Y., KOJIMA, M., SATO, N. and KIKUCHI, T. (1992): Development of imaging riometers. Nankyoku Shiryô (Antarct. Rec.), **36**, 227–250 (in Japanese with English abstract).

YAMAGISHI, H., FUJITA, Y., SATO, N., STAUNING, P., NISHINO, M. and MAKITA, K. (1998): Conjugate features of auroras observed by TV cameras and imaging riometers at auroral zone and polar cap conjugate-pair stations. Polar Cap Boundary Phenomena, ed. by J. MOEN *et al.* Dordrecht, Kluwer A.P., 289–300.

(Received December 1, 1997; Revised manuscript accepted January 21, 1998)